




# Effects of chronic voluntary alcohol consumption on PDE10A availability: a longitudinal behavioral and [ $^{18}\text{F}$ ]JNJ42259152 PET study in rats

Bart de Laat<sup>1</sup> · Yvonne E. Kling<sup>2,3</sup> · Gwen Schroyen<sup>4</sup> · Maarten Ooms<sup>5</sup> · Jacob M. Hooker<sup>6</sup> · Guy Bormans<sup>5</sup> · Koen Van Laere<sup>1,7</sup> · Jenny Ceccarini<sup>1,8</sup> 

Received: 8 March 2021 / Accepted: 3 June 2021 / Published online: 17 June 2021  
© The Author(s), under exclusive licence to Springer-Verlag GmbH Germany, part of Springer Nature 2021

## Abstract

**Purpose** Phosphodiesterase 10A (PDE10A) is a dual substrate enzyme highly enriched in dopamine-receptive striatal medium spiny neurons, which are involved in psychiatric disorders such as alcohol use disorders (AUD). Although preclinical studies suggest a correlation of PDE10A mRNA expression in neuronal and behavioral responses to alcohol intake, little is known about the effects of alcohol exposure on in vivo PDE10A activity in relation to apparent risk factors for AUD such as decision-making and anxiety.

**Methods** We performed a longitudinal [ $^{18}\text{F}$ ]JNJ42259152 microPET study to evaluate PDE10A changes over a 9-week intermittent access to alcohol model, including 6 weeks of alcohol exposure, 2 weeks of abstinence followed by 1 week relapse. Parametric PDE10A-binding potential ( $\text{BP}_{\text{ND}}$ ) images were generated using a Logan reference tissue model with cerebellum as reference region and were analyzed using both a volume-of-interest and voxel-based approach. Moreover, individual decision-making and anxiety levels were assessed with the rat Iowa Gambling Task and open-field test over the IAE model.

**Results** We observed an increased alcohol preference especially in those animals that exhibited poor initial decision-making. The first 2 weeks of alcohol exposure resulted in an increased striatal PDE10A binding ( $> 10\%$ ). Comparing PDE10A-binding potential after 2 versus 4 weeks of exposure showed a significant decreased PDE10A in the caudate-putamen and nucleus accumbens ( $p_{\text{FWE-corrected}} < 0.05$ ). This striatal PDE10A decrease was related to alcohol consumption and preference. Normalization of striatal PDE10A to initial levels was observed after 1 week of relapse, apart from the globus pallidus.

**Conclusion** This study shows that chronic voluntary alcohol consumption induces a reversible increased PDE10A enzymatic availability in the striatum, which is related to the amount of alcohol preference. Thus, PDE10A-mediated signaling plays an important role in modulating the reinforcing effects of alcohol, and the data suggest that PDE10A inhibition may have beneficial behavioral effects on alcohol intake.

**Keywords** Alcohol preference · Phosphodiesterase 10A · MicroPET · [ $^{18}\text{F}$ ]JNJ42259152 · Open-field test · Rat Iowa Gambling Task

---

Bart de Laat and Yvonne E. Kling contributed equally to this work.

---

This article is part of the Topical Collection on Preclinical Imaging.

---

✉ Jenny Ceccarini  
jenny.ceccarini@uzleuven.be

Extended author information available on the last page of the article

## Introduction

Alcohol use disorders (AUD) have a large impact on the population's mental and physical well-being as they embody chronically relapsing conditions with relapse rates of 40–60%. It is now commonly accepted that addiction develops through phases, characterized by an initial recreational use, followed by excessive consumption, compulsive drug seeking and episodic withdrawal, and terminates in drug seeking and relapse. However, although the knowledge on the neurobiology of AUD is still expanding, efficacious treatments for AUD are still missing.

Aside from classical targets associated with alcohol-related reward, such as dopaminergic, glutamatergic, mu-opioid, and GABAergic neurons [1–3], research is now also focusing on biological substrates responsible for negative reinforcement and chronic relapse, impulse loss of control, dysphoria, anxiety, stress, and maladaptive mechanisms resulting from protracted drug use.

Specific subclasses of the phosphodiesterase (PDE) enzyme family are particularly attractive for pharmacological manipulation in respect to drugs of abuse, including alcohol [4]. PDEs are dual specific enzymes which hydrolyze cyclic adenosine and guanosine monophosphate (cAMP and cGMP), consequently regulating cognate signaling pathways such as synaptic plasticity [5], learning, memory, and cognition [6, 7] as well as promoting neuronal survival [8]. Several studies suggested the cyclic nucleotide phosphodiesterase-10A (PDE10A) as a promising target when it comes to tackling diseases that have been related with disturbances of striatal dopamine transmission like neurodegenerative and neuropsychiatric disorders [9], due to its high and localized expression in the medium spiny neurons (MSNs) of the basal ganglia [10]. PDE10A is involved in the hydrolysis of the cyclic nucleotides adenosine monophosphate (cAMP) and guanosine monophosphate (cGMP) [11, 12], regulating the excitability of MSNs and thereby acting on the postsynaptic dopaminergic neurotransmission. Both dopamine D1 and D2 receptors mediate their effects through activation or inactivation of the cAMP/PKA (protein kinase A) pathway in the MSNs [13]. PDE10A can thus be seen as a key regulator of basal ganglia dopaminergic function [9].

In line with this, several studies have shown that changes in dopamine neurotransmission are related to changes in PDE10A activity [14–16]. Pharmacological inhibition of PDE10A has been shown preclinical and clinical efficacy in movement-related disorders such as Parkinson's and Huntington's diseases [17–22], but also in neuropsychiatric diseases such as schizophrenia [6, 23–25] and substance use disorders [26, 27]. For instance, MP-10, a highly selective PDE10A inhibitor, attenuates morphine-induced conditioned place preference and facilitates extinction in rats [26], similarly to cocaine-induced effects [27].

In AUD, PDE10A has been suggested to also be a regulator of neuronal responses after reinforcement and to alter motivated behaviors like alcohol self-administration. The first connection between PDE10A and AUD was established when PDE10A mRNA expressions in the prelimbic prefrontal cortex showed a correlation with greater alcohol self-administration during the relapse-like phase in rats with a history of stress exposure [28]. Secondly, during protracted withdrawal, PDE10A mRNA levels were reduced in the dorsal striatum, prelimbic prefrontal cortex, and medial amygdala, in contrary to elevated PDE10A mRNA expression observed in the basolateral amygdala during both acute and

protracted withdrawal [29]. The same group also showed administration of TP-10, another selective PDE10A inhibitor, was able to reduce alcohol self-administration in alcohol-dependent and non-dependent rats with or without a history of stress and in genetically alcohol-preferring rats [30].

Whereas there is preclinical evidence to support the involvement of PDE10A in neuronal and behavioral responses to alcohol intake and preference, little is known about the effects of alcohol exposure, abstinence, and relapse on *in vivo* PDE10A enzymatic activity, in relation to apparent risk factors for AUD such as decision-making and anxiety. To address this knowledge gap, we performed a longitudinal [ $^{18}\text{F}$ ]JNJ42259152 PDE10A microPET imaging [31] study, to directly measure *in vivo* changes of PDE10A availability in rats monitored over a 9-week alcohol abuse reinstatement model, mimicking different stages of AUD, in combination with decision-making and anxiety assessments.

## Materials and methods

### Animals and procedures

In total, 18 adult male Wistar rats (R. Janvier, Le Genest-St-Isle, France), individually housed in a temperature- and humidity-controlled room under an inverse 12-h light/dark cycle, were investigated (average weight at the time of the experiment:  $332 \pm 7$  g). Only male rats were included in the study in view of the known gender effect in the availability or expression of PDE10A [32–34]. A subset of 9 experimental animals were monitored over a 9-week intermittent access of ethanol model (described in the following paragraph), including 6 weeks of alcohol exposure, 2 weeks of abstinence followed by 1 week relapse. The other group of 9 rats were included as a sham group (water exposure) to mainly evaluate the differences of chronic alcohol exposure on PDE10A enzymatic activity compared to baseline levels.

### Alcohol drinking paradigm

An intermittent access 20% ethanol 2-bottle choice drinking paradigm, adapted from Simms et al. [35], referred to as an “intermittent access to ethanol” (IAE) animal model, was employed to induce alcohol intake as described previously [36]. The IAE animal model is highly relevant to early stages of alcohol abuse and is one of the most prominent animal models used in ethanol research [37]. Every 24 h, the paradigm was changed presenting either 2 drinking bottles, a water and an experimental ethanol solution bottle containing a 20% v/v dilution of 99% v/v percent stock ethanol (Technisolv, VWR chemicals, Radnor, PA, USA). After 24 h, both bottles were taken away and replaced by a single water bottle. To avoid side preference bias, drinking bottles were

alternated [35] and bottles were weighted 24 h after delivery. Alcohol consumption and alcohol preference, calculated as the ratio between the solution and water consumption, were used as outcome. After 6 weeks of alcohol exposure, the rats underwent 2 weeks of abstinence phase with access to the bottle of water only. Finally, the rats regained access during a second alcohol exposure period to alcohol for 1 week to mimic relapse. A detailed timeline of the experiment is shown in Fig. 1.

## Behavioral testing

Decision-making and anxiety-related behavior were assessed in all experimental animals with the rat Iowa Gambling Task (rIGT) (adapted from Zeeb et al. [38]) and open-field test (OFT) at week 0 (baseline); weeks 1, 3, 6 (ethanol exposure phase); weeks 7 and 8 (abstinence phase), and at week 9 (relapse phase) (Fig. 1). An extensive description of the behavioral tasks is reported in the [Supplementary Material](#). Briefly, for the rIGT, the outcome (decision-making score) was calculated as [(no. pellets rewarded/no. nose-pokes)], with 2 equals to efficient decision-making and < 1.8 equals to poor decision-making. The reinforcement schedule was designed so that the two-pellet choice was optimal in terms of reward earned per unit time. Animals received weekly testing sessions and each session lasted 30 min. The total number of trials completed, i.e. amount of times an animal successfully poked its nose in an illuminated hole, were analyzed as a fraction of the total pellets received, as a measurement of risk-taking behavior. In low risk-taking behavior, this number approximates two, indicating primarily option two was chosen. Animal's individual anxiety-related behavior was assessed using the OFT. Each animal was placed in the center of an open field apparatus that consists of a standard circle arena with a diameter of 80 cm, height 31.5 cm, surrounded by a 40 cm rim. The ratio between the average center distance over the total distance from the edge to the center was used as surrogate marker for anxiety: a lower locomotor activity was interpreted as a more anxious state.

Behavioral tests were always executed on the first 2 days of the week, in the same order, on similar hours throughout the day starting after 3 h from the last access to the drinking bottles to allow robust comparison between groups.

## Small animal PET imaging: acquisition and analysis

Small animal PDE10A imaging was performed using [ $^{18}\text{F}$ ]JNJ42259152. [ $^{18}\text{F}$ ]JNJ42259152 is a potent and highly selective inhibitor of PDE10A. JNJ-42259152 inhibits the cAMP-hydrolyzing activity of purified recombinant PDE10A with potency pIC<sub>50</sub> (known log of inhibition constant at 50%) of 8.82 for the human enzyme [39]. In vitro binding affinity of [ $^{18}\text{F}$ ]JNJ42259152 is  $K_D = 6.62 \pm 0.7$  nM [40]. The radiotracer was obtained with a radiochemical purity > 98% and an average molar activity of 150 GBq/ $\mu\text{mol}$  at the time of injection.

PDE10A scans were performed on a Focus 220 microPET scanner (Siemens Medical Solutions, Knoxville, TN, USA), which has a transaxial resolution of 1.35 mm in full-width at half maximum. The entire scan, rats were kept under gas anesthesia (2.5% isoflurane in O<sub>2</sub> at a flow rate of 1 L/min) and on a heating pad at 37 °C. Heart rate and breathing rate of all rats were monitored during the entire experiment. Animals were injected intravenously into the tail vein with an average of  $24.1 \pm 1.9$  MBq ( $23.4 \pm 1.8$  MBq at the first time point,  $24.8 \pm 1.8$  MBq at the second time point, and  $24.0 \pm 2.2$  MBq at the last time point).

Dynamic 60-min scans started simultaneously with [ $^{18}\text{F}$ ]JNJ42259152 injection with 3 animals scanned on a single bed at the same time. Celen et al. [41] previously demonstrated that for a 60-min dynamic micro-PET acquisition, striatal BP of the intact tracer referenced to the cerebellum showed very good correlation with corresponding BP values of a simplified reference tissue model and referenced Logan Plot. Data were acquired in a  $128 \times 128 \times 95$  matrix with a pixel width of 0.95 mm and a slice thickness of 0.8 mm. List-mode data were reconstructed in 21 time frames ( $4 \times 15$  s,  $4 \times 60$  s,  $5 \times 180$  s,  $8 \times 300$  s) for a 60-min acquisition using an iterative maximum a posteriori probability algorithm reconstruction and attenuation correction by means of  $^{57}\text{Co}$ -attenuation scan. A summed image of the reconstructed data was spatially normalized to a custom-made rat brain template ( $^{11}\text{C}$ -raclopride) in Paxinos stereotactic space [42], which also has a predominant striatal uptake. The affine transformation was then used to normalize all time frames of the dynamic micro-PET data set to allow automated and symmetric volumes of interest (VOI) analyses, using a

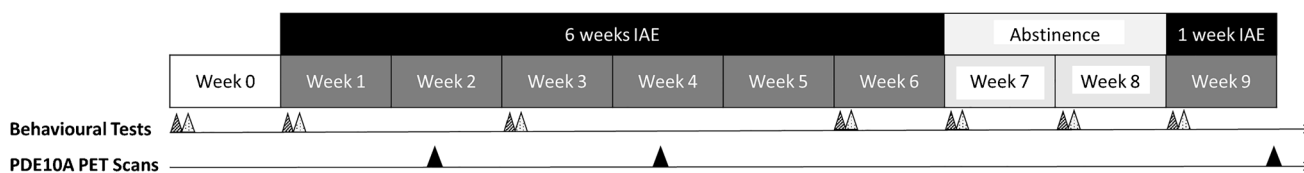


**Fig. 1** Schematic overview of the experimental design. Time-course of the 9 weeks of the intermittent access of ethanol (IAE) animal model, indicating the time points of the behavioral tests (gray triangle

with black stripes for open-field test (OFT), white triangle with black points for rat Iowa Gambling Task (rIGT)) and PDE10A microPET scans (black triangle)

predefined VOI map defined in PMOD (v3.3; PMOD Technologies, Zürich, Switzerland). Parametric PDE10A-binding potential ( $BP_{ND}$ ) images were generated using a Logan reference tissue model with cerebellum as reference region [31, 40], and were analyzed using both a VOI- and voxel-based approach. Parametric PDE10A  $BP_{ND}$  images of the 9 rats used as a control sham group [40] to facilitate comparison with the 2-week alcohol exposure experimental group were generated using the acquisition time interval of 60 min and were identically processed.

Voxel-wise analyses were performed without a priori knowledge of the target regions using Statistical Parametric Mapping 12 (SPM12, Wellcome Department of Cognitive Neurology, London, UK). After spatial normalization, PDE10A  $BP_{ND}$  images were smoothed with a 1.2-mm full width at half maximum Gaussian filter and masked for extracerebral signals. SPM analysis of PDE10A  $BP_{ND}$  data was performed with an 80% relative analysis threshold in a flexible factorial design for longitudinal data, and in a categorical design for the control group versus each alcohol condition. *T*-map thresholds were set at 0.005 uncorrected for the peak voxel level and  $> 200$  voxels for the cluster size (kE). Only clusters that reached significance at  $p_{cluster} < 0.05$  (FWE corrected) were retained.

## Statistical analysis

Conventional statistics were carried out using GraphPad Prism 8.1.2 software (GraphPad Software Inc., La Jolla, CA, USA). A nonparametric Friedman test followed by a Dunn's post hoc test was performed to detect differences on the alcohol consumption and alcohol preference across the different weeks of alcohol exposure. The same statistical test

was performed to compare  $BP_{ND}$  values at the different time points. An unpaired Mann–Whitney *t*-test was performed to evaluate  $BP_{ND}$  changes in the experimental alcohol group compared to the sham control condition, for both VOI- and voxel-based analysis. We explored correlations between regional PDE10A changes between the different alcohol conditions and behavioral outcomes using Spearman's non-parametric test. Data are expressed as the mean  $\pm$  SEM, and statistical significance was set at  $p < 0.05$ .

## Results

### Alcohol consumption and preference

Overall, both alcohol consumption and preference significantly increased over time (alcohol consumption:  $\chi^2(6) = 42.77$ ,  $p < 0.0001$ ; alcohol preference:  $\chi^2(6) = 43.39$ ,  $p < 0.0001$ ). The alcohol consumption significantly escalated at week 3 ( $p < 0.05$ ), as well as at week 6 ( $p < 0.0001$ ) and week 9 (relapse condition;  $p < 0.0001$ ) in comparison to the initial intake reported at week 1 (Fig. 2a). Compared to week 1 (average  $2.8 \pm 0.6$  g/kg/day), the rats reached a higher alcohol consumption (76%) after only 3 weeks of administration ( $4.9 \pm 0.7$  g/kg/day). After 2 weeks of abstinence, the alcohol consumption remained overall stable ( $6.0 \pm 1.0$  g/kg/day) (Fig. 2a). Similarly, alcohol preference (alcohol/water) increased over time with significantly higher preference during week 3 ( $32 \pm 5\%$ ;  $p < 0.005$ ) and during the relapse period ( $33 \pm 6\%$ ;  $p < 0.005$ ), compared to week 1 (Fig. 2b). Noteworthy, we observed that few rats developed higher alcohol consumption and preference during the first phase

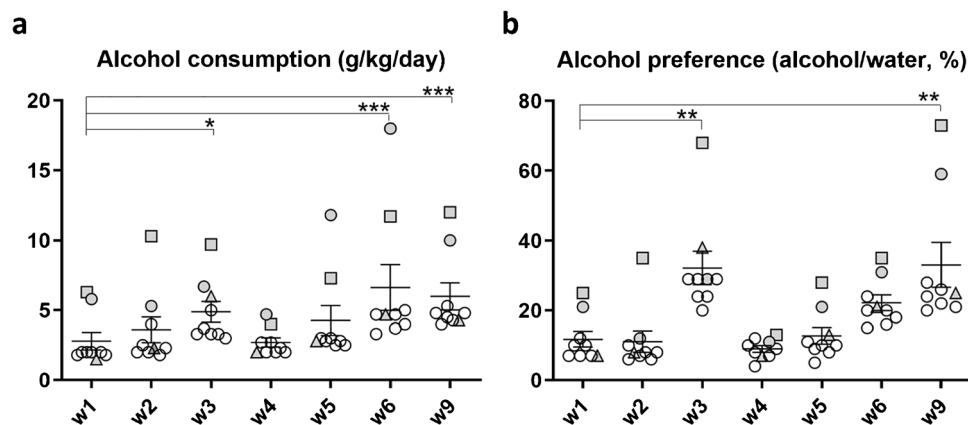


**Fig. 2** Alcohol consumption and preference in function of the alcohol exposure week. Aligned dot plots (mean  $\pm$  SEM) showing weekly **a** average alcohol (g/kg/day) consumption and **b** alcohol preference (%; ratio of volume alcohol solution/water intake) over a period of 9 weeks of the intermittent access of ethanol (IAE) animal model.

Filled gray symbols show those rats who reported a higher alcohol consumption above the mean during at week 3 of the IAE model. W, week; \* $p < 0.05$ ; \*\* $p < 0.005$ ; \*\*\* $p < 0.0001$  (Dunn's nonparametric comparison for post hoc Friedman test)

of the IAE model, which was maintained or even increased after abstinence.

## Behavioral testing

### Rat Iowa Gambling Task

Assessing risk-taking behavior during the 9 weeks of alcohol model, the rIGT revealed overall a general constant behavioral performance across the IAE model. The mean decision-making score was  $1.90 \pm 0.08$ . The rats obtained  $70 \pm 5$  rewards consisting of  $132 \pm 7$  pellets in total. We could not observe significant alcohol-related changes in risk-taking performances ( $p=0.12$ ). However, when looking at baseline individual rIGT performance, a subgroup of rats scored low ranging from 1.4 to 1.7 (on average  $1.6 \pm 0.1$ ; Fig. 3a). To evaluate whether individual behavioral baseline characteristics of the animals had an influence on their alcohol consumption, mixed model analysis was performed. The score on the rIGT was shown to significantly predict alcohol consumption over time ( $p=0.017$ ). When dividing the animals based on the baseline rIGT score ( $<1.8$  vs.  $>1.8$  equals to poor vs. normal decision-making) and displaying their alcohol consumption, a significant difference between the two groups was observed exclusively at baseline ( $p<0.001$ ). Indeed, the rats scoring low on the baseline rIGT ( $<1.8$ ) were those rats who consumed a larger and increasing amount of alcohol per day (Fig. 3a).

### Open-field test

The IAE model displayed an overall main effect on the two OFT outcome automated measures over the different alcohol phases compared to baseline, determined by both the

mean total distance traveled ( $p<0.0001$ ) as well as the distance to the center ( $p<0.0001$ ), and hence by the resulting center distance/total distance ratio during the 10 min OFT ( $p<0.0001$ ). This applied to all time points when comparing to baseline ( $67.4 \pm 2.9$  cm), resulting in a significant decreased locomotor activity during the 6 weeks of chronic-alcohol intake ( $33.5 \pm 4.5$  cm), the abstinence phase (weeks 7 and 8;  $30.6 \pm 2.6$  cm) and relapse (week 9;  $27.5 \pm 3.2$  cm) (Fig. 3b). The OFT ratio significantly decreased during the relapse phase (reflecting an increased anxious behavior), comparing to week 3 and 6 of alcohol consumption ( $p=0.02$ , Fig. 3c). While baseline OFT characteristics could not predict initial alcohol consumption (interaction effects), significant effect of the alcohol consumption on OFT performances was observed during the final alcohol intake period ( $p=0.037$ ), the first week of abstinence ( $p=0.022$ ) and relapse (week 9;  $p=0.003$ ).

### PDE10A microPET changes and alcohol exposure

Average PDE10A  $BP_{ND}$  maps acquired for the sham control condition and for the experimental IAE condition (after 2, 4 weeks of alcohol exposure, and at relapse after 2 weeks of abstinence) are represented in Fig. 4a. The first 2 weeks of alcohol exposure (ALC w2) resulted in an increased PDE10A binding in the striatum ( $+12\%$ ,  $p=0.04$ ; Fig. 5), compared to the sham group. Voxel-based comparison between sham and ALC w2 revealed increased PDE10A  $BP_{ND}$  values in two clusters comprising the bilateral caudate-putamen ( $p_{\text{height}}<0.005$ ; Fig. 4b).

Comparing PDE10A  $BP_{ND}$  after 4 versus 2 weeks of exposure, showed a decreased PDE10A binding in the bilateral caudate-putamen, extending to the NuAc shell and bed nucleus of the stria terminalis ( $P_{\text{FWE-corrected}}$ :

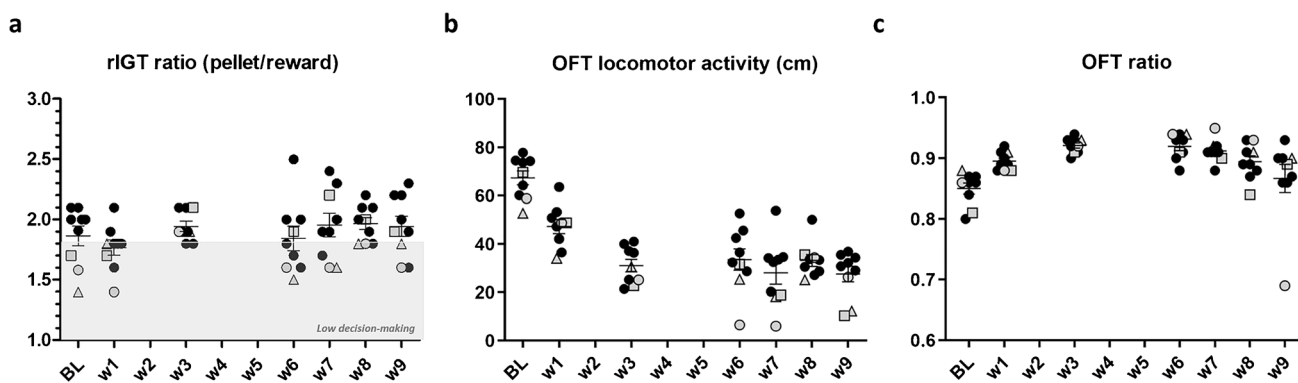


**Fig. 3** Behavioral outcome (rat Iowa Gambling Task (rIGT) and open-field test (OFT)) in function of the alcohol exposure week and alcohol consumption. Aligned dot plots (mean  $\pm$  SEM) showing the weekly **a** mean ratio of rewards/pellets for the rat Iowa Gambling Task (rIGT) measuring the decision-making and risk-taking, **b** the mean total distance (in cm), and **c** center distance/total distance ratio

traveled during the 10 min OFT, over a period of 9 weeks of the intermittent access of ethanol (IAE) animal model. The gray symbols correspond to the same rats who reported a high alcohol consumption and preference during the first IAE phase. \* $p<0.05$  Dunn's nonparametric comparison for post hoc Friedman test

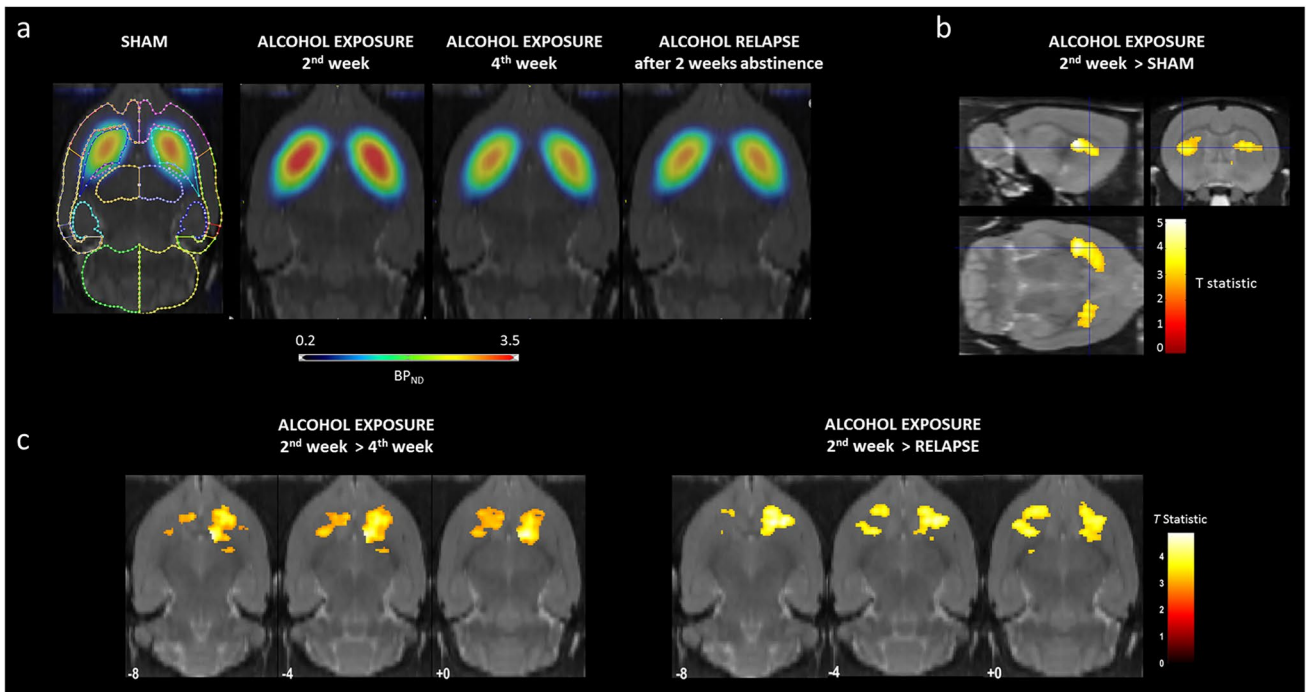


**Fig. 4** Phosphodiesterase 10a (PDE10A) availability changes at 2 and 4 weeks of alcohol exposure, and during the relapse phase. **a** Merged striatal PDE10A availability at the time points of control (sham), alcohol exposure week 2, alcohol week 4, and relapse shows the initial increase of PDE10A availability in alcohol week 2 and its reversibility over alcohol week 4 and no increase at relapse conditions. Additionally, an illustrative example of the volumes-of-interest (VOI) map in Paxinos space is presented in Fig. 4a. **b** Brain sections

show overlays of *T*-maps at the voxel level on the striatal regions with significantly increased PDE10A availability after 2 weeks of alcohol exposure, compared to sham. The intersection point is set to the Paxinos coordinate peak max ( $p=2.5 \cdot 10^{-4}$ ) located in the left caudate-putamen ( $x=-4.4$  mm,  $y=0.7$  mm,  $z=4.6$  mm). **c** PDE10A decreased in a cluster located in the bilateral caudate-putamen and NuAc comparing 2 weeks and 4 weeks alcohol exposure as well as 2 weeks vs. 2 weeks relapse alcohol exposure

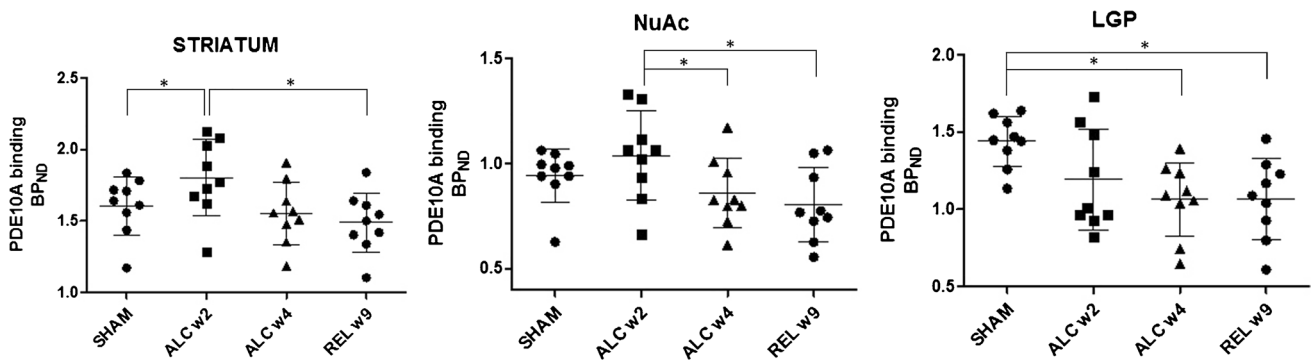


**Fig. 5** PDE10A binding in rats after 1 week of relapse compared to the sham control group. Brain sections show overlays of *T*-maps on the regions with significantly decreased PDE10A binding after 1 week of relapse, compared to the sham control group. The intersec-

tion point is set to the Paxinos coordinate located in the right globus pallidum ( $x=3.0$  mm,  $y=-0.9$  mm,  $z=5.8$  mm,  $p=0.001$ ,  $T=3.2$ ). Significant clusters are indicated using a *T*-statistic color scale, which shows significance at the voxel level

0.02–0.003,  $T_{\text{peak}} > 3.6$ , Fig. 4c; VOI-based: striatum:  $-14\%$ ,  $\chi^2(2)=8.22$ ,  $p=0.02$ ; NuAc:  $-17\%$ ,  $\chi^2(2)=8.67$ ,  $p=0.01$ ).

A similar regional decrease in PDE10A availability towards normalization was observed after 2 weeks of abstinence, extending to the lateral globus pallidum ( $P_{\text{FWE-corrected}}: 0.002-0.008$ ,  $T_{\text{peak}} > 3.8$ , Fig. 4c; VOI-based:

striatum:  $-17\%$ ,  $p=0.02$ ; NuAc:  $-22\%$ ,  $p=0.01$ ). After 1 week of relapse, VOI-based analysis confirmed this PDE10A augmentation back to PDE10A binding at sham condition in the striatum ( $p=0.19$ ) and NuAc ( $p=0.14$ ). VOI- and voxel-based analyses showed that the decreased PDE10A availability in the lateral globus pallidum at week

2 of alcohol exposure tends to further decrease at week 4 and relapse, extending to the bed nucleus of the stria terminalis ( $p_{\text{height}} < 0.005$ ; mean decrease =  $-29 \pm 14\%$  at Paxinos coordinate:  $x = 3.0$ ,  $y = -0.9$ ,  $z = 5.8$ ; VOI-based:  $p = 0.004$ , see Figs. 4 and 5).

The observed alcohol-induced striatal PDE10A changes were not related to rIGT performances at any time point of the alcohol model. It is nevertheless noteworthy that no significant alcohol-related changes in risk-taking performances were observed over time (see Fig. 3a). However, comparing the percentage changes of the OFT locomotor activity over the different alcohol phases with individual baseline performances, our explorative correlation analyses revealed negative correlations between PDE10A binding changes in the NuAc at week 4 of alcohol exposure and during relapse and decrease in OFT locomotor activity at the initial and final phase of the alcohol model (alcohol week 1:  $r_s = -0.7$ ;  $p = 0.043$ ; relapse period week 9:  $r_s = -0.65$ ;  $p = 0.05$ ).

## Discussion

In the current preclinical study, we combined longitudinal behavioral paradigms with longitudinal PDE10A micro PET imaging, to directly evaluate in vivo changes of PDE10A activity in rats during different stages of AUD, in combination with behavioral assessments such as anxiety and decision-making. Overall, we found that 2 weeks of voluntary alcohol consumption induced a reversible increased PDE10A enzymatic availability in the dorsal and ventral striatum. At both week 4 of the alcohol exposure and relapse, the striatal PDE10A decrease was related to alcohol consumption and preference. Also, the rats who showed a greater future alcohol intake corresponded to those rats with an initial impaired decision-making and a lower locomotor activity, possibly due to a more anxious state, during the abstinence and relapse phase.

To induce alcohol consumption in our experimental group of rats, we used the IAE model with a 2-bottle choice paradigm, one of the most prominent and validated animal models used in ethanol research nowadays [35, 37]. The IAE model successfully induced an escalation in alcohol consumption after the first weeks of alcohol administration, following the threshold criteria of high ethanol consumption ( $> 4.5$  g/kg/day) suggested by Carnicella et al. [43]. Moreover, after the 2 weeks of abstinence, the average alcohol intake returned to the same level as before the period of abstinence, suggesting that IAE paradigm induces adaptations which are maintained after abstinence, in line with previous findings [35, 43]. However, although half of the group did not exploit high alcohol consumption during the first intake phase, observing the progress of the individual ethanol intake, a subgroup of rats clearly developed high

alcohol consumption over time. So far, little is known about the predisposing behavioral traits of high alcohol intake in rats, except rats with higher impulsivity traits are known to have a higher alcohol intake [44]. Noteworthy, in this study, a low baseline rIGT performance, hence impaired initial decision-making, is related to a higher alcohol consumption over time. When looking at behavioral outcomes in function of the alcohol exposure over time; 6 weeks of alcohol intake had no effects on decision-making performances, while on the other hand a decreased locomotor activity (hence increased anxious behavior) was found starting from week 3 on, including the abstinence and relapse period.

Regarding alcohol consumption and PDE10A availability over time, our longitudinal [ $^{18}\text{F}$ ]JNJ42259152 PDE10A imaging data showed that two weeks of voluntary alcohol consumption induced an increased PDE10A enzymatic availability in the striatum. We also found that this alcohol-induced PDE10A upregulation was reversible upon a longer period of alcohol administration and was mostly present in those rats that consumed a bigger amount of alcohol. A similar regional decrease in PDE10A availability towards normalization was observed after one week of relapse, extending to the lateral globus pallidum. These findings are in line with previous PDE10A PET findings by Tollefson et al. obtained in recently abstinent cocaine users [45], where  $\text{BP}_{\text{ND}}$  values were lower in the globus pallidus in cocaine users relative to controls. The observed PDE10A changes might be a result of alterations in dopamine neurotransmission and subsequent PDE10A modulation through feedback on the cAMP/PKA pathway. PDEs can promote alcohol intake through reduction of cyclic nucleotide activity [46]. Considering the limited distribution of PDE10A to the striatal GABAergic MSNs, together with the role of PDE10A in cAMP-PKA-DARPP-32 signaling cascade and metabolism in the MSNs, several studies have demonstrated a relation between abnormal striatal dopaminergic transmission characterizing neurodegenerative and neuropsychiatric basal ganglia diseases and the loss of PDE10A enzyme levels and expression [18, 21–23, 27]. Upregulated striatal signaling, is PDE10A-regulated in processes controlling reward-motivated behaviors and furthermore, incentive salience [47]. In the striatum, the increased dopamine release upon alcohol exposure stimulates both the dopamine D1 and D2 receptor pathways in the postsynaptic density of the MSNs resulting in increased (via D1) or decreased (D2) cAMP levels. It is of central question whether our findings are mostly a consequence of increased stimulation of the direct D1 pathway, or via the opposite indirect D2 pathway resulting in the activation of  $\text{G}\alpha_{i/o}$ , and cAMP inhibition. Ooms et al. [16] observed increased PDE10A binding after repeated D-amphetamine treatment, suggesting a potential pharmacological interaction between PDE10A enzymes and drugs modifying dopamine neurotransmission. This was

suggested to be a compensation mechanism secondary to alterations of cAMP levels being caused by increased D1 receptor stimulation over D2 stimulation. Here, we showed that PDE10A availability in the striatum increases at the first stage of alcohol exposure (week 2) and then gradually decreases. Also, the striatal PDE10A decrease observed between 4 and 2 weeks was mostly present in high alcohol-preferring rats, compared to the low alcohol-preferring rats (Supplemental Fig. 1). This might indicate a short-term neuronal adaptation due to alcohol-induced increased dopamine release, which results in increased stimulation of adenylyl cyclase and thus increased cAMP levels. The MSNs react to increased cAMP levels by up-regulating cyclic nucleotide hydrolyzing enzymes. As a consequence, this leads to an increased PDE10A enzymatic availability that subsequently decreases cAMP levels. Due to the long-term chronic alcohol effect, dopamine release decreases [48–51] leading to less cAMP production and to a loss of PDE10A. Since we did not observe an increased PDE10A availability during the relapse phase after abstinence, this suggests neuroadaptational changes within specific neurocircuits take place in a long-term fashion.

Preclinical studies suggested that pharmacological inhibition of PDE10A activity with TP-10 dose-dependently reduce alcohol self-administration in rats with stress history, alcohol dependence, or genetic predisposition to high levels of alcohol intake [30]. This action may result, at least partially, from modulation of PDE10A activity in the dorsolateral striatum (DLS), the region that showed a non-recovered PDE10A loss in our findings. Furthermore, systemic TP-10 administration significantly increased dopamine turnover in the DLS and NuAc, with greater potency in the DLS [52]. Consistently, PDE10A inhibition reduces intake of highly palatable high-fat diets in mice [53], supporting PDE10A is involved in the motivational regulation of highly reinforcing substances.

Our findings suggest that it may be a therapeutic target of interest at the initial stage of AUD. Further research is required to advance our understanding of these findings. There is no increase in PDE10A signal after relapse and therefore, we hypothesize an irreversible neuroadaptational change has taken place due to the MSNs down-regulating cyclic nucleotide hydrolyzing enzymes, such as PDE10A. This provides further insight into the molecular mechanisms that are at play in alcoholism and that are so crucial to be fully understood in order to tackle alcoholism as a disease.

The negative emotional state that arises during acute abstinence from alcohol exposure includes elevations in anxiety-like behavior [54]. Previous studies showed that PDE10A may mediate the relation between stress history and elevated relapse risk [28]. Papaverine, a PDE10A inhibitor, has been shown to reduce anxiety-like behavior [55]. Stress history differentially increased PDE10A

expression in low versus high drinking rats, with greater PDE10A expression in the prefrontal cortex correlating with greater relapse-like alcohol intake, and greater PDE10A expression in the basolateral amygdala correlating with increased alcohol preference ratios in rats [28]. In agreement with these findings, our results showed that those rats with decreased locomotor activity over the first initial alcohol and relapse phase and therefore, increased anxiety levels, displayed reduced PDE10A changes during both the protracted alcohol exposure (4 weeks) and relapse. This indicates elevated PDE10A levels are associated with heightened anxiety-like behavior. On the other hand, our correlation findings are pure exploratory and need further validations. Also, anxiety is a complex collection of behaviors and aspects that cannot be entirely captured by a single test. Although it would be interesting to confirm our findings using other testing, such as the elevated plus maze (EPM) or the light/dark boxes (LDB). Factor analyses revealed that similar anxiety- and locomotion-related factors were produced by the three tests OFT, EPM and LDB applied either separately or in combination [56].

Our study was of exploratory nature, and we investigated male rats. Evidence in humans highlights the importance of a different brain physiology in AUD depending on sex, as summarized in the review of Ceylan-Isik et al. [57]. Importantly, receptor density differences have been detected between sexes in striatal D2 receptor density [58]. In the future it would be interesting to examine a mixed, bigger group to reveal any possible striatal PDE10A density differences among sexes.

A limitation of our study is the small group size of animals used in this study. Increasing the number of animals would help to improve characterization of the subgroups divided by high and low alcohol consumption. Another potential limitation is the lack of the pre-exposure baseline PDE10A measurements, resulting in only limited information on studying the dynamics of PDE10A changes occurring during exposure to alcohol. Nevertheless, a sham control group scanned under the same conditions was used to investigate the effect of chronic alcohol administration. Moreover, although sham animals were not subjected to behavioral tasks, limiting therefore the interpretability of the current behavioral data, the validation of both OFT and rIGT tests was obtained in a FDG PET sub-study (data not shown). Finally, future research will be needed to correlate our findings to the exact underlying molecular mechanisms, for example by validating protein or RNA expression level changes of PDE10A, as for example shown in the study by Logrip et al. [29] which showed reduced mRNA PDE10A expression in dorsal striatum during withdrawal. This would also be very interesting in regard of cAMP/PKA pathway-related targets.



To our knowledge, this is the first PDE10A microPET study investigating in vivo changes of PDE10A activity in rats during different stages of AUD, in relation to apparent risk factors for AUD such as decision-making and anxiety. Our findings indicate that chronic alcohol consumption induces a reversible increased PDE10A enzymatic availability in the striatum that is related to higher alcohol preference. Secondly, we showed that poor decision-making (i.e. high risk-taking and gambling-prone behavior) may be a predisposing factor for a higher vulnerability towards alcohol abuse and AUD, and decreased locomotor activity (i.e. increased anxiety) may be a consequence of chronic alcohol use. Thus, PDE10A-mediated signaling plays an important role in modulating the reinforcing effects of alcohol, and the data suggest that PDE10A inhibition may have beneficial behavioral effects on alcohol intake.

**Abbreviations** AUD: Alcohol use disorders; BP: Binding potential; cAMP: Cyclic adenosine monophosphate; cGMP: Cyclic guanosine monophosphate; D1: Dopamine receptor type 1; D2: Dopamine receptor type 2; IAE: Intermittent access to ethanol; MSNs: Medium spiny neurons; NuAc: Nucleus accumbens; OFT: Open-field test; PDE: Phosphodiesterase; PDE10A: Phosphodiesterase 10A; rIGT: Rat Iowa Gambling Task; VOI: Volumes of interest

**Supplementary Information** The online version contains supplementary material available at <https://doi.org/10.1007/s00259-021-05448-3>.

**Acknowledgements** The authors would like to thank Tinne Buelens and Ann Van Santvoort for their excellent technical assistance and the local radiopharmacy team for the tracer productions.

**Authors' contributions** The experimental setup was designed by BdL and JC. BdL, GS and MO performed data collection. Data analysis was conducted by YEK and JC. The manuscript was written by YEK and JC, supported by BdL, GS, MO, JMH, GB and KVL. All authors revised the manuscript and accepted the final version.

**Funding** This work was funded by a research grant to JC from the Research Foundation Flanders (FWO/1508415 N). JC is a postdoctoral fellow from FWO (FWO/12R1619N). YEK is a SB PhD fellow at FWO (FWO/1S50320N), BdL received a PhD fellowship from the Flemish Agency for Innovation by Science and Technology, and KVL is senior clinical research fellow for the FWO. GS, MO, JMH, and GB have no competing financial interests to report in relation to this work.

**Data availability of data and materials** Please contact the authors for data request.

## Declarations

**Ethics approval** All animal experiments were conducted according to the European Communities Council Directive of November 24, 1986 (86/609/EEC) and approved by the Animal Ethics Committees of the University of Leuven.

**Competing interests** The authors declare that they have no competing interests.

## References


1. Leurquin-Sterk G, Ceccarini J, Crunelle CL, Weerasekera A, de Laat B, Himmelreich U, et al. Cerebral dopaminergic and glutamatergic transmission relate to different subjective responses of acute alcohol intake: an in vivo multimodal imaging study. *Addict Biol.* 2018;23:931–44.
2. de Laat B, Weerasekera A, Leurquin-Sterk G, Gsell W, Bormans G, Himmelreich U, et al. Effects of alcohol exposure on the glutamatergic system: a combined longitudinal  $^{18}$ F-FPEB and  $^1$ H-MRS study in rats. *Addic Biol.* 2019;24:696–706.
3. Xiao C, Ye JH. Ethanol dually modulates GABAergic synaptic transmission onto dopaminergic neurons in ventral tegmental area: role of  $\mu$ -opioid receptors. *Neuroscience.* 2008;153:240–8.
4. Logrip ML. Phosphodiesterase regulation of alcohol drinking in rodents. *Alcohol.* 2015;49:795–802.
5. Sanderson TM, Sher E. The role of phosphodiesterases in hippocampal synaptic plasticity. *Neuropharmacology.* 2013;74:86–95.
6. García-Barroso C, Ugarte A, Martínez M, Rico AJ, Lanciego JL, Franco R, et al. Phosphodiesterase inhibition in cognitive decline. *J Alzheimers Dis.* 2014;42:S561–73.
7. Peng S, Sun H, Zhang X, Liu G, Wang G. Effects of selective phosphodiesterases-4 inhibitors on learning and memory: a review of recent research. *Cell Biochem Biophys.* 2014;70:83–5.
8. Kranz K, Warnecke A, Lenarz T, Durisin M, Scheper V. Phosphodiesterase type 4 Inhibitor rolipram improves survival of spiral ganglion neurons in vitro. Sokolowski B, editor. *PLoS One.* 2014;9:e92157.
9. Wilson L, Brandon N. Emerging Biology of PDE10A. *Curr Pharm Des.* 2014;21:378–88.
10. Seeger TF, Bartlett B, Coskran TM, Culp JS, James LC, Krull DL, et al. Immunohistochemical localization of PDE10A in the rat brain. *Brain Res.* 2003;985:113–26.
11. Jäger R, Russwurm C, Schwede F, Genieser H-G, Koesling D, Russwurm M. Activation of PDE10 and PDE11 phosphodiesterases. *The Journal of biological chemistry.* *J Biol Chem.* 2012;287:1210–9.
12. Gross-Langenhoff M, Hofbauer K, Weber J, Schultz A, Schultz JE. cAMP is a ligand for the tandem GAF domain of human phosphodiesterase 10 and cGMP for the tandem GAF domain of phosphodiesterase 11. *The Journal of biological chemistry.* *J Biol Chem.* 2006;281:2841–6.
13. Nishi A, Kuroiwa M, Miller DB, O'Callaghan JP, Bateup HS, Shuto T, et al. Distinct roles of PDE4 and PDE10A in the regulation of cAMP/PKA signaling in the striatum. *J Neurosci.* 2008;28:10460–71.
14. Dlaboga D, Hajjhussein H, O'Donnell JM. Chronic haloperidol and clozapine produce different patterns of effects on phosphodiesterase-1B, -4B, and -10A expression in rat striatum. *Neuropharmacol.* 2008;54:745–54.
15. Giorgi M, Melchiorri G, Nuccetelli V, D'Angelo V, Martorana A, Sorge R, et al. PDE10A and PDE10A-dependent cAMP catabolism are dysregulated oppositely in striatum and nucleus accumbens after lesion of midbrain dopamine neurons in rat: a key step in parkinsonism physiopathology. *Neurobiol Dis.* 2011;43:293–303.
16. Ooms M, Celen S, De Hoogt R, Lenaerts I, Liebrechts J, Vanhoof G, et al. Striatal phosphodiesterase 10A availability is altered secondary to chronic changes in dopamine neurotransmission. *EJNMMI Radiopharm Chem.* 2017;1:3.
17. Niccolini F, Foltynie T, Reis Marques T, Muhlert N, Tziortzi AC, Searle GE, et al. Loss of phosphodiesterase 10A expression is associated with progression and severity in Parkinson's disease. *Brain.* 2015;138:3003–15.

18. Pagano G, Niccolini F, Wilson H, Yousaf T, Khan NL, Martino D, et al. Comparison of phosphodiesterase 10A and dopamine transporter levels as markers of disease burden in early Parkinson's disease. *Movement Disord.* 2019;34:1505–15.
19. Beaumont V, Zhong S, Lin H, Xu W, Bradaia A, Steidl E, et al. Phosphodiesterase 10A inhibition improves cortico-basal ganglia function in Huntington's disease models. *Neuron.* 2016;92:1220–37.
20. Wilson H, Niccolini F, Haider S, Marques TR, Pagano G, Coello C, et al. Loss of extra-striatal phosphodiesterase 10A expression in early premanifest Huntington's disease gene carriers. *J Neurol Sci.* 2016;368:243–8.
21. Koole M, Van Laere K, Ahmad R, Ceccarini J, Bormans G, Vandenberghe W. Brain PET imaging of phosphodiesterase 10A in progressive supranuclear palsy and Parkinson's disease. *Movement Disord.* 2017;32:943–5.
22. Ahmad R, Bourgeois S, Postnov A, Schmidt ME, Bormans G, Van Laere K, et al. PET imaging shows loss of striatal PDE10A in patients with Huntington disease. *Neurology.* 2014;82:279–81.
23. Persson J, Szalicszyó K, Antoni G, Wall A, Fällmar D, Zora H, et al. Phosphodiesterase 10A levels are related to striatal function in schizophrenia: a combined positron emission tomography and functional magnetic resonance imaging study. *Eur Arch Psychiatry Clin Neurosci.* 2020;270:451–9.
24. Bodén R, Persson J, Wall A, Lubberink M, Ekselius L, Larsson E-M, et al. Striatal phosphodiesterase 10A and medial prefrontal cortical thickness in patients with schizophrenia: a PET and MRI study. *Transl Psychiatry.* 2017;7:e1050.
25. Chappie T, Humphrey J, Menniti F, Schmidt C. PDE10A inhibitors: an assessment of the current CNS drug discovery landscape. *Curr Opin Drug Discov Devel.* 2009;12:458–67.
26. Mu Y, Ren Z, Jia J, Gao B, Zheng L, Wang G, et al. Inhibition of phosphodiesterase 10A attenuates morphine-induced conditioned place preference. *Mol Brain.* 2014;7:70.
27. Liddle S, Anderson KL, Paz A, Itzhak Y. The effect of phosphodiesterase inhibitors on the extinction of cocaine-induced conditioned place preference in mice. *J Psychopharmacol.* 2012;26:1375–82.
28. Logrip ML, Zorrilla EP. Stress history increases alcohol intake in relapse: relation to phosphodiesterase 10A. *Addict Biol.* 2012;17:920–33.
29. Logrip ML, Zorrilla EP. Differential changes in amygdala and frontal cortex Pde10a expression during acute and protracted withdrawal. *Front Integr Neurosci.* 2014;8:30.
30. Logrip ML, Vendruscolo LF, Schlosburg JE, Koob GF, Zorrilla EP. Phosphodiesterase 10A regulates alcohol and saccharin self-administration in rats. *Neuropsychopharmacology.* 2014;39:1722–31.
31. Celen S, Koole M, Ooms M, De Angelis M, Sannen I, Cornelis J, et al. Preclinical evaluation of [18F]JNJ42259152 as a PET tracer for PDE10A. *Neuroimage.* 2013;82:13–22.
32. Logrip ML, Gainey SC. Sex differences in the long-term effects of past stress on alcohol self-administration, glucocorticoid sensitivity and phosphodiesterase 10A expression. *Neuropharmacology.* 2020;164:107857. <https://doi.org/10.1016/j.neuropharm.2019.107857>.
33. Hsu YT, Liao G, Bi X, Oka T, Tamura S, Baudry M. The PDE10A inhibitor, papaverine, differentially activates ERK in male and female rat striatal slices. *Neuropharmacology.* 2011;61:1275–81.
34. Fazio P, Schain M, Mrzljak L, Amini N, Nag S, Al-Tawil N, et al. Patterns of age related changes for phosphodiesterase type-10A in comparison with dopamine D2/3 receptors and sub-cortical volumes in the human basal ganglia: A PET study with 18F-MNI-659 and 11C-raclopride with correction for partial volume effect. *Neuroimage.* 2017;152:330–9.
35. Simms JA, Steensland P, Medina B, Abernathy KE, Chandler LJ, Wise R, et al. Intermittent access to 20% ethanol induces high ethanol consumption in Long-Evans and Wistar rats. *Alcohol Clin Exp Res.* 2008;32:1816–23.
36. Laat B, Weerasekera A, Leurquin-Sterk G, Gsell W, Bormans G, Himmelreich U, et al. Effects of alcohol exposure on the glutamatergic system: a combined longitudinal 18F-FPEB and 1H-MRS study in rats. *Addict Biol.* 2019;24:696–706.
37. Kimbrough A, Kim S, Cole M, Brennan M, George O. Intermittent access to ethanol drinking facilitates the transition to excessive drinking after chronic intermittent ethanol vapor exposure. *Alcohol Clin Exp Res.* 2017;41:1502.
38. Zeeb FD, Robbins TW, Winstanley CA. Serotonergic and dopaminergic modulation of gambling behavior as assessed using a novel rat gambling task. *Neuropsychopharmacol.* 2009;34:2329–43.
39. Van Laere K, Ahmad RU, Hudyana H, Dubois K, Schmidt ME, Celen S, et al. Quantification of 18F-JNJ-42259152, a novel phosphodiesterase 10A PET tracer: Kinetic modeling and test-retest study in human brain. *J Nucl Med.* 2013;54:1285–93.
40. Ooms M, Attili B, Celen S, Koole M, Verbruggen A, Van Laere K, et al. [18F]JNJ42259152 binding to phosphodiesterase 10A, a key regulator of medium spiny neuron excitability, is altered in the presence of cyclic AMP. *J Neurochem.* 2016;139:897–906.
41. Celen S, Koole M, De Angelis M, Sannen I, Chitneni SK, Alcazar J, et al. Preclinical evaluation of 18F-JNJ41510417 as a radioligand for PET imaging of phosphodiesterase-10A in the brain. *J Nucl Med.* 2010;51:1584–91.
42. Casteels C, Vermaelen P, Nuyts J, Van Der Linden A, Baekelandt V, Mortelmans L, et al. Construction and evaluation of multitracer small-animal PET probabilistic atlases for voxel-based functional mapping of the rat brain. *J Nucl Med.* 2006;47:1858–66.
43. Carnicella S, Ron D, Barak S. Intermittent ethanol access schedule in rats as a preclinical model of alcohol abuse. *Alcohol.* 2014;48:243–52.
44. Poulos CX, Le AD, Parker JL. Impulsivity predicts individual susceptibility to high levels of alcohol self-administration. *Behav Pharmacol.* 1995;6:810–4.
45. Tollefson S, Gertler J, Himes ML, Paris J, Kendro S, Lopresti B, et al. Imaging phosphodiesterase-10a availability in cocaine use disorder with [11 C]JMA107 and PET. *Synapse.* 2019;73:e22070.
46. Wen R-T, Zhang F-F, Zhang H-T. Cyclic nucleotide phosphodiesterases: potential therapeutic targets for alcohol use disorder. *Psychopharmacology.* 2018;235(6):1793–805. <https://doi.org/10.1007/s00213-018-4895-7>.
47. Piccart E, De Backer J-F, Gall D, Lambot L, Raes A, Vanhoof G, et al. Genetic deletion of PDE10A selectively impairs incentive salience attribution and decreases medium spiny neuron excitability. *Behav Brain Res.* 2014;268:48–54.
48. Narendran R, Mason NS, Paris J, Himes ML, Douaihy AB, Frankle WG. Decreased prefrontal cortical dopamine transmission in alcoholism. *Am J Psychiatry.* 2014;171:881–8.
49. Volkow ND, Wang G-J, Telang F, Fowler JS, Logan J, Jayne M, et al. Profound decreases in dopamine release in striatum in detoxified alcoholics: possible orbitofrontal involvement. *J Neurosci.* 2007;27:12700–6.
50. Martinez D, Gil R, Slifstein M, Hwang D-R, Huang Y, Perez A, et al. Alcohol dependence is associated with blunted dopamine transmission in the ventral striatum. *Biol Psychiat.* 2005;58:779–86.
51. Heinz A, Siessmeier T, Wrase J, Buchholz HG, Gründer G, Kumakura Y, et al. Correlation of alcohol craving with striatal dopamine synthesis capacity and D2/3 receptor availability: a combined [18F]DOPA and [18F]DMFP PET study in detoxified alcoholic patients. *Am J Psychiatry.* 2005;162:1515–20.

52. Schmidt CJ, Chapin DS, Cianfrogna J, Corman ML, Hajos M, Harms JF, et al. Preclinical characterization of selective phosphodiesterase 10a inhibitors: a new therapeutic approach to the treatment of schizophrenia. *J Pharmacol Exp Ther.* 2008;325:681–90.
53. Nawrocki AR, Rodriguez CG, Toolan DM, Price O, Henry M, Forrest G, et al. Genetic deletion and pharmacological inhibition of phosphodiesterase 10A protects mice from diet-induced obesity and insulin resistance. *Diabetes.* 2014;63:300–11.
54. Zhao Y, Weiss F, Zorrilla EP. Remission and resurgence of anxiety-like behavior across protracted withdrawal stages in ethanol-dependent rats. *Alcoholism: Clin Exp Res.* 2007;31:1505–15.
55. Grauer SM, Pulito VL, Navarra RL, Kelly MP, Kelley C, Graf R, et al. Phosphodiesterase 10A inhibitor activity in preclinical models of the positive, cognitive, and negative symptoms of schizophrenia. *J Pharmacol Exp Ther.* 2009;331:574–90.
56. Ramos A, Pereira E, Martins GC, Wehrmeister TD, Izídio GS. Integrating the open field, elevated plus maze and light/dark box to assess different types of emotional behaviors in one single trial. *Behav Brain Res.* 2008;193:277–88.
57. Ceylan-Isik AF, McBride SM, Ren J. Sex difference in alcoholism: Who is at a greater risk for development of alcoholic complication? *Life Sci* 2010;87(5–6):133–8. <https://doi.org/10.1016/j.lfs.2010.06.002>
58. Pohjalainen T, Rinne JO, Nägren K, Syvälahti E, Hietala J. Sex differences in the striatal dopamine D2 receptor binding characteristics in vivo. *Am J Psychiatry.* 1998;155:768–73.

**Publisher's note** Springer Nature remains neutral with regard to jurisdictional claims in published maps and institutional affiliations.

## Authors and Affiliations

Bart de Laat<sup>1</sup> · Yvonne E. Kling<sup>2,3</sup> · Gwen Schroyen<sup>4</sup> · Maarten Ooms<sup>5</sup> · Jacob M. Hooker<sup>6</sup> · Guy Bormans<sup>5</sup> · Koen Van Laere<sup>1,7</sup> · Jenny Ceccarini<sup>1,8</sup> 

<sup>1</sup> Nuclear Medicine and Molecular Imaging, Department of Imaging and Pathology, KU Leuven, Leuven, Belgium

<sup>2</sup> Department of Neurosciences, KU Leuven, Experimental Neurology and Leuven Brain Institute (LBI), Leuven, Belgium

<sup>3</sup> Center for Brain & Disease Research, Laboratory of Neurobiology, VIB, Leuven, Belgium

<sup>4</sup> Department of Imaging and Pathology, Translational MRI, KU Leuven, Leuven, Belgium

<sup>5</sup> Laboratory for Radiopharmaceutical Research, KU Leuven, Leuven, Belgium

<sup>6</sup> Athinoula A. Martinos Center for Biomedical Imaging, Department of Radiology, Massachusetts General Hospital, Harvard Medical School, Charlestown, MA, USA

<sup>7</sup> Division of Nuclear Medicine, University Hospitals Leuven, Leuven, Belgium

<sup>8</sup> University Hospitals Leuven, Herestraat 49, 3000 Leuven, Belgium